JOURNAL OF MAGNETIC RESONANCE **131,** 254–260 (1998)
ARTICLE NO. MN981359

Radiofrequency-Driven and Slow-Magic-Angle-Sample-Spinning Polarization-Transfer Techniques: A Comparative Study

P. Robyr and Z. Gan

Laboratorium für Physikalische Chemie, ETH-Zentrum, CH-8092 Zürich, Switzerland

Received September 2, 1997; revised December 19, 1997

The rate constant of radiofrequency-driven (RF-driven) polarization transfer and that of polarization transfer under slow-magic-angle sample spinning (S-MAS) are compared using a model system, polycrystalline α-α'-$^{13}C_2$-phthalic acid. While the rate constant under RF irradiation in static samples strongly depends on the orientation of the internuclear vector, the rate constant under S-MAS is hardly sensitive to that orientation and, thus, depends almost exclusively on the internuclear distance. Consequently, polarization-transfer rate constants obtained under S-MAS can be interpreted more simply when used to study local order in polycrystalline or amorphous solids. © 1998 Academic Press

Key Words: **solid state NMR; polarization transfer; spin diffusion; RF-driven; S-MAS.**

INTRODUCTION

Transfer of nuclear spin polarization, often termed spin diffusion, can provide detailed information about the local structure in solids (*1–13*). It is especially useful for studying amorphous solids and can well complement scattering techniques in crystalline systems. One application of nuclear polarization transfer is the determination of the relative orientation of molecular fragments. This can be achieved by correlating the relative orientation of chemical shielding anisotropy (CSA) tensors of neighboring nuclei using two-dimensional nuclear magnetic resonance (2D NMR) spectroscopy (*14–16*).

Proton-driven polarization transfer (*4–9*) has been used to measure relative orientations between inequivalent sites in polycrystalline solids. In these 2D experiments, the time during which polarization transfer occurs is chosen long enough so that a quasi-equilibrium state is reached (*10*). The corresponding quasi-equilibrium spectra contain no information on distances between inequivalent sites but suffice to extract the relative orientation of CSA tensors. If the system under study is amorphous and, thus, contains at most short range order, the quasi-equilibrium spectrum does not provide any detail about the relative orientations. Structural information must be retrieved from the rates at which the polarization is transferred from one spin to its neighbors (*10*).

The rate constants of polarization transfer of the proton-driven technique often strongly depend on the resonance frequencies of the two spins involved in the transfer process (*10*). This dependency makes the extraction of structural information from the rate constants difficult. Polarization-transfer techniques, which do not suffer from this problem, have been developed. Radiofrequency (RF)-driven polarization transfer (*17*) uses a strong pulsed spin-lock field which, in the rotating frame, scales down the effective resonance-frequency difference below the homogeneous width of the zero-quantum (ZQ) line. Typically, this technique can eliminate the dependence of polarization transfer on resonance frequency over a chemical shift range of 10 kHz using a RF field strength of about 100 kHz (*10, 12*). More recently, polarization transfer under slow-magic-angle sample spinning (S-MAS) was proposed (*18*). Here, the resonance-frequency difference during polarization transfer is modulated by slowly rotating the sample about an axis at a magic angle respective to the static magnetic field. For spin pairs with equal isotropic values of their CSA tensors the resonance-frequency difference always changes its sign during a full rotation about the magic angle axis, so that polarization transfer averaged over a rotor cycle is efficient for all spin pairs. It was shown that polarization transfer under S-MAS becomes independent of resonance-frequency over a range wider than that covered by RF-driven spin diffusion (*18*). Indeed, it is so wide that polarization transfer between deuterons with quadrupolar coupling constants up to 100 kHz can easily be observed (*21, 22*).

This paper focuses on the different behavior of polarization transfer under RF-driven and S-MAS conditions. As derived from perturbation theory, the rate constant of polarization transfer between two spins depends on the square of their dipolar coupling (*23–25*). The two techniques affect the dipolar couplings in different ways. The application of the RF field approximately halves the strength of the dipolar interactions, while the rotation of the sample under S-MAS causes a modulation of the angle between the internuclear vector and the static magnetic field and, consequently, a modulation of the dipolar couplings. To illustrate the consequence of this difference, measurements in ^{13}C-labeled phthalic acid at the two carboxylic groups are presented. On the basis of these measurements and of corresponding

1090-7807/98 $25.00

calculations, it is shown that S-MAS modulation leads to average rate constants which depend almost exclusively on the distance between the spins. The consequence of the difference between the two polarization-transfer techniques is discussed in view of investigating local order in amorphous solids. In the course of this comparative study, the orientation of the carboxylic ^{13}C CSA tensor with respect to the molecular frame in phthalic acid was determined.

THEORETICAL BACKGROUND

We consider two coupled spins, $S = \frac{1}{2}$, whose energy levels are broadened by coupling to additional spins, such that the homogeneous linewidth of the broadened levels is larger than the dipolar coupling between the two spins. Then, the rate constant of polarization transfer between the two spins i and j is given by (*23*)

$$W_{ij} = \tfrac{1}{2}\pi s_{ij}^2 b_{ij}^2 F_{ij}(0), \qquad [1]$$

where s_{ij} is a scaling factor, b_{ij} the dipolar coupling between spin i and spin j, and $F_{ij}(0)$ the intensity of the normalized zero-quantum spectrum sampled at frequency zero. The scaling factor is $s_{ij} = 1$ for polarization transfer with the magnetization stored along the static magnetic field (proton-driven, S-MAS), and approaches $s_{ij} = -0.5$ for RF-driven polarization transfer in the case of efficient spin-lock sequences (*10, 12*). The dipolar coupling b_{ij} depends on the internuclear distance r_{ij}, and on the angle between the internuclear vector and the static magnetic field θ_{ij}

$$b_{ij} = -\frac{\mu_0 \gamma_S^2 \hbar}{4\pi r_{ij}^3}\left(\frac{3\cos^2\theta_{ij} - 1}{2}\right), \qquad [2]$$

where γ_S is the gyromagnetic ratio. The intensity of the normalized ZQ spectrum $F_{ij}(0)$ corresponds to the intensity of the ZQ line sampled at $\Omega_i - \Omega_j$ from its maximal value, where Ω_i and Ω_j are the resonance frequencies of spin i and spin j.

Two-dimensional NMR spectroscopy of polycrystalline or amorphous samples cannot provide the rate constant of polarization transfer between particular spins, but it yields the rate constant as a function of the resonance frequencies of the spins that exchange their polarization. In the initial rate approximation, an average rate constants W_{AB} can be defined

$$W_{AB} = \langle \tfrac{1}{2}\pi s_{ij}^2 b_{ij}^2 F_{ij}(0)\rangle_{AB}, \qquad [3]$$

where $\langle \cdots \rangle_{AB}$ stands for the average over all pairs with the particular resonance frequencies Ω_A and Ω_B. It is important to note that the average rate constant W_{AB} is defined in the initial rate approximation (*10*) and, consequently, must be measured from the initial slope of the crosspeak intensities.

In RF-driven polarization transfer, the scope of the spin-lock sequence is to reduce the effective resonance-frequency difference of the irradiated spins to a value much smaller than the homogeneous width of the ZQ line, so that $F_{ij}^{\mathrm{RF}}(0)$ will coincide with the central value of the line (*10, 12*). In addition, the spin-lock sequence decouples the S spins from possible heteronuclear spins, yielding narrowed ZQ lines and correspondingly higher $F_{ij}^{\mathrm{RF}}(0)$ values. For a homonuclear spin system in which each pair of neighbors is surrounded by several other spins, the width of the ZQ line does not vary appreciably with the resonance frequencies Ω_i and Ω_j, and consequently, $F_{ij}^{\mathrm{RF}}(0)$ will virtually take the same value, $F^{\mathrm{RF}}(0)$, over the whole range of resonance frequency. The dipolar coupling b_{ij} is left unaffected by the RF irradiation, the scaling of the dipolar interactions is accounted for by the factor s_{ij}. For efficient spin-lock sequences $s_{ij} \approx -0.5$ (*10, 12*), and the rate constant W_{AB}^{RF} becomes

$$W_{AB}^{\mathrm{RF}} = \tfrac{1}{8}\pi \langle b_{ij}^2 \rangle_{AB} F^{\mathrm{RF}}(0). \qquad [4]$$

In polarization transfer under S-MAS, the sample rotation modulates the resonance frequencies, Ω_i and Ω_j, and the dipolar coupling b_j (Eq. [2]). The rotation frequency is selected to be small compared to the homogeneous linewidth of the ZQ line but higher than the polarization transfer rate constants, so that a rate constant averaged over one rotation period can be calculated from the instantaneous values taken by b_{ij} and $F_{ij}^H(0)$ during one rotor cycle (*18*). We have

$$\bar{W}_{ij} = \tfrac{1}{2}\pi \overline{b_{ij}^2 F_{ij}^H(0)}, \qquad [5]$$

where the bar stands for the average of the static values over one rotor period, and $F_{ij}^H(\omega)$ is the ZQ spectrum of the spin pair i and j under the coupling to the protons. The rate constant $\bar{W}_{AB}$, evaluated from the intensity at (Ω_A, Ω_B) in the 2D spectrum is

$$\bar{W}_{AB} = \tfrac{1}{2}\pi \langle \overline{b_{ij}^2 F_{ij}^H(0)} \rangle_{AB}. \qquad [6]$$

The average over all spin pairs with the particular resonance frequencies Ω_A and Ω_B in Eqs. [4] and [6] can include pairs with different relative orientation of their CSA tensors and also pairs with different orientation of the internuclear vector with respect to the static field. These types of degeneracy cannot be used to simplify the calculation of the average rate constants without making assumptions about the structure under investigation. However, for polarization transfer under S-MAS in polycrystalline samples or in unoriented amorphous systems, there is one additional degeneracy which arises from the absence of macroscopic order. All spin pairs related by a rotation about the static magnetic

field contribute to the same rate constant $\bar{W}_{AB}$, but the trajectories of the dipolar coupling and those of the resonance frequencies during a rotor cycle differ for different pairs. Consequently, enhanced transfer due to small resonance frequency differences happens for many different instantaneous values of θ_{ij}. A general evaluation of the average rate constant is not possible, but if the ZQ spectrum is known, the rate constant for a given geometry can be calculated. A set of such calculations allows the evaluation of the maximal deviation from an ideal situation where the averaging leaves the rate of polarization transfer independent of the angular part of the dipolar coupling. In this situation, the rate constant can be written as

$$\bar{W}_{AB} = \frac{\pi}{10}\left(\frac{\mu_0 \gamma_S^2 \hbar}{4\pi}\right)^2 \langle r_{ij}^{-6}\rangle_{AB} \langle \overline{F_{ij}^H(0)}\rangle_{AB}. \qquad [7]$$

The ZQ term $\langle \overline{F_{ij}^H(0)}\rangle_{AB}$ can be evaluated as proposed in Ref. (*18*). Usually, it hardly depends on the resonance frequencies. In a forthcoming section, it will be shown that even for the most stringent case with a unique relative orientation of the CSA tensors and a unique orientation of the internuclear vector with respect to the CSA tensors, Eq. [7] is a reasonable approximation.

EXPERIMENTAL

The measurements were performed on α-α'-$^{13}C_2$-phthalic acid ($^{13}C > 99\%$) (Isotech, OH) using a home-built spectrometer working at a proton frequency of 300 MHz. The 2D polarization-transfer experiments followed the general scheme of 2D exchange spectroscopy (*16*). Carbon coherences are prepared by cross-polarization from the protons. They freely precess during the evolution period under proton decoupling. Then, polarization transfer takes place during the mixing time, where one component of the transverse magnetization is stored along the *z* axis for transfer under S-MAS or spin-locked in the rotating frame for RF-driven transfer. Finally, the carbon coherences are detected under proton decoupling.

The S-MAS data were obtained with a Chemagnetics (Fort Collins, CO) 6-mm double-resonance MAS probe as discussed previously (*18*). The MAS frequency was 100 ± 1 Hz. The RF fields on the ^{13}C and the ^{1}H channels were both matched at 62 kHz.

The RF-driven polarization-transfer spectra were obtained with a Chemagnetics (Fort Collins, CO) 4-mm double-resonance MAS probe. The probe was operated in the static mode with both radiofrequency channels for ^{13}C and ^{1}H matched at 100 kHz. The mixing sequence consisted of a WALTZ17 sequence (*19*) on the ^{13}C channel with simultaneous homonuclear decoupling of the protons using a BLEW12 sequence (*20*). The duration of the 17th pulse of the WALTZ sequence corresponded to a flip angle of 90°.

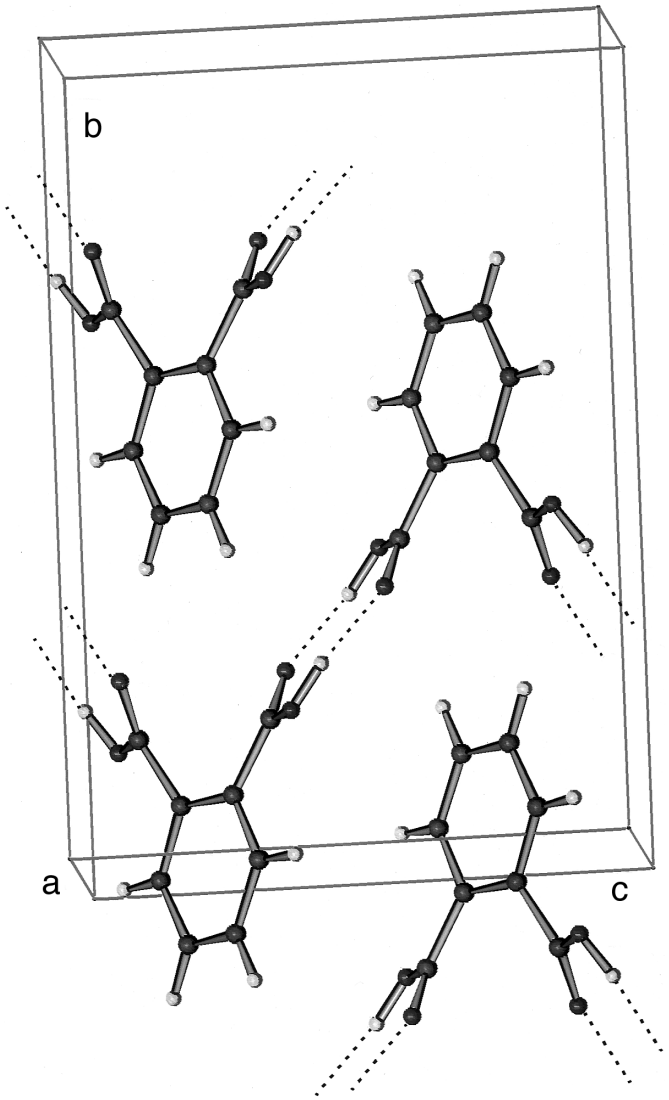

FIG. 1. Unit cell of phthalic acid. The crystal structure is monoclinic and belongs to the space group $C2/c$, with a = 5.0698 Å, b = 14.3178 Å, c = 9.6305 Å, and β = 93.260°. The structure consists of infinite chains of hydrogen-bonded molecules.

The 2D separated-local-field spectrum (*26*), needed to evaluate the ZQ spectra under S-MAS, was obtained from a 2D experiment with zero mixing time and without decoupling during the evolution period.

PHTHALIC ACID

The unit cell of phthalic acid belongs to the space group $C2/c$ and consists of infinite chains of hydrogen-bonded molecules (Fig. 1) (*27, 28*). A twofold rotation axis transforms each half of a molecule into the other, and thus also relates the two ^{13}C CSA tensors of the carboxylic groups. The four molecules in the unit cell are related in pairs by

inversion symmetries so that in a crystallite only two different orientations of the carboxylic groups exist. The distance between the two carboxylic carbons in the same molecule is 3.05 Å. The next shortest distance between inequivalent sites is 4.10 Å. The closest equivalent neighbor is at 3.82 Å in the nearest hydrogen-bonded molecule. Consequently, since the rate of polarization transfer decreases with the sixth power of the distance, the exchange of polarization in the initial rate regime is confined almost exclusively to the two inequivalent sites in the same molecule. This restriction allows us to investigate and compare the dependence of the rate constants on the angular part of the dipolar coupling in RF-driven and S-MAS polarization transfer. Before focusing on the rate constants of polarization transfer, the relative orientation of the two carboxylic ^{13}C CSA tensors and their orientation in a molecule-fixed frame shall be characterized.

ORIENTATION OF THE ^{13}C CSA TENSORS

From the quasi-equilibrium spectrum of Fig. 2a, the relative orientation between the two carboxylic ^{13}C CSA tensors of the same molecule can be obtained (*8, 14, 15*). Determining this orientation is equivalent to positioning the twofold symmetry (C_2) axis in one of the two principal axis systems (PAS) of the CSA tensors. The analysis was performed in two steps. First, the homogeneous line, assumed to be a 2D Gaussian function, and the eigenvalues of the CSA tensors were determined by least-squares fitting of a 2D spectrum with zero mixing time. We obtained δ_{xx} = 238.4 ppm, δ_{yy} = 165.5 ppm, and δ_{zz} = 100.6 ppm (from TMS), and for the width of the 2D Gaussian function 1010 Hz. In a second step, the 2D spectrum of Fig. 2a was fitted to determine the polar angles, θ_c and ϕ_c, of the C_2 axis in the PAS of the CSA tensor as shown in Fig. 3. The fit yielded θ_c = 58.7° ± 1.0° and ϕ_c = 56.5° ± 1.0°.

From the orientation of the C_2 axis in the PAS of the CSA tensor, it is not possible to unequivocally orient the CSA tensor in a molecule fixed frame (*8*). The relation between the two frames can only be determined up to a rotation about the C_2 axis. To discuss this problem further, it is convenient to define a molecular frame with its z_m axis perpendicular to the (OCO) plane, its y_m axis along the C═O bond, and its x_m axis pointing in the direction of the nearest hydrogen-bonded molecule as sketched in Fig. 3. According to empirical rules (*29, 30*), the most shielded direction of the CSA tensor should be perpendicular to the carboxylic plane, and thus coincides with the z_m axis. However, the information obtained so far constrains the *z* axis of the CSA tensor to lie on a cone about the C_2 axis with aperture θ_c (Fig. 3). Selecting the smallest angle between the *z* axis of the CSA tensor and that of the molecular frame consistent with this restriction, one can obtain the orientation of CSA tensor in the molecular frame. The resulting set of Euler angles (α, β, γ) relating the two frames is (56.2°, −3.5°, −58.6°). This

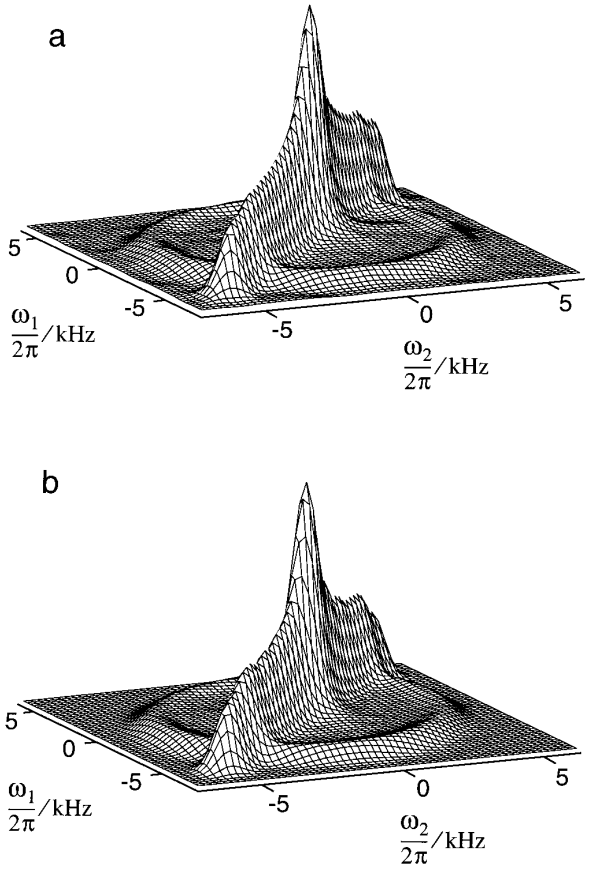

FIG. 2. (a) Two-dimensional quasi-equilibrium polarization-transfer spectrum of α-α'-$^{13}C_2$-phthalic acid obtained under slow-magic-angle sample spinning using a mixing time of 200 ms. (b) Best computer fit of the spectrum (a). In the least-squares fit, the polar angles θ_c and ϕ_c, which orient the twofold symmetry axis in the principal axis system of the CSA tensor of the carboxylic carbon, are optimized. We obtained θ_c = 58.7° ± 1.0° and ϕ_c = 56.5° ± 1.0°.

transformation approximately corresponds to an orientation of the CSA tensor where its *z* axis is tilted by 3.5° in the direction of the nearest hydrogen-bonded molecule.

Another possibility to orient unequivocally the CSA tensor in the molecular frame is to use the rate constants of polarization transfer measured with the RF-driven technique (Fig. 4a). Assuming that $F_{ij}^{RF}(0) = F^{RF}(0)$, the rate constants of Fig. 4a can be fitted to Eq. [4]. Two parameters were optimized in a least-squares fit: $F^{RF}(0)$ and Ψ, the angle of the rotation about the C_2 axis that generates all possible orientations of the CSA tensor in the molecular frame consistent with the values obtained for θ_c and ϕ_c (Fig. 3). We obtained Ψ = 4.9° ± 7.0° and $F^{RF}(0) = (1.98 \pm 0.01) \times 10^{-4}$ s. The value of Ψ agrees with the nominal value of zero derived from the empirical rule. The rate constants yielded by the fit are shown in Fig. 4b. The overall agreement between the experimental and the calculated rate constants is good. However, significant deviations occur.

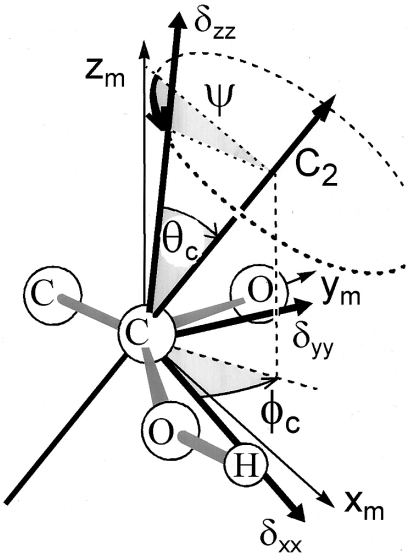

FIG. 3. Schematic representation of the angles θ_c, ϕ_c, and Ψ. The polar angles θ_c and ϕ_c define the orientation of the twofold symmetry (C_2) axis in the principal axis system of the CSA tensor of the carboxylic carbon. The molecular frame (x_m, y_m, z_m) is defined such that its z_m axis is perpendicular to the OCO plane and its y_m axis is along the C═O bond. In combination with the angles θ_c and ϕ_c, the rotation of angle ψ about the C_2 axis defines unequivocally the orientation of the CSA tensor in the molecular frame. For $\Psi = 0°$ the z axis of the CSA tensor is in the plane defined by the C_2 axis and the z_m axis.

They are partially reflected in the large errors for the parameter Ψ. Most probably, these deviations are due to the simplicity of the model used to calculate the rate constants. The model considers only the coupling b_{ij} between two nearest S spins explicitly; the other couplings among the S spins are assumed to broadened the energy levels of the two neighbors so that the broadening is larger than the coupling b_{ij} and independent of the resonance frequencies of the two neighbors. This type of model can describe the spin dynamics of homonuclear systems with dominant dipolar couplings only to a limited accuracy.

RATE CONSTANTS OF POLARIZATION TRANSFER

The rate constants of polarization transfer measured under RF-driven conditions vary from 20 to 330 s^{-1} (Fig. 4a). The variation is due to a correlation between the resonance frequencies and the orientation of the $^{13}C-^{13}C$ vector with respect to the static magnetic field. This orientation is a determinant for the strength of the dipolar coupling, and consequently, for the rate of polarization transfer.

The rate constants measured using S-MAS are shown in Fig. 4c. Their mean value is 11.5 s^{-1} and their variations are confined within ±13%. The rate constants $\bar{W}_{AB}$ can be calculated from Eq. [6] using the orientation of the CSA tensor in the molecular frame determined above. The intensities of the ZQ spectra $F_{ij}^{H}(0)$ can be approximately evaluated from the cross-product of two one-quantum spectra (*31*, *32*). These are obtained from sections along ω_1 in the 2D separated-local-field spectrum (*26*) shown in Fig. 5. The calculated rate constants are displayed in Fig. 4d. The mean value is 15.5 s^{-1} and the variations are between ±19%. Their mean value is 30% higher than that of the experimental data (Fig. 4c). Nevertheless, if the distance between the two carboxylic carbons is calculated from the experimental rate constants, the obtained value, 3.23 Å, is only 6% larger than that mea-

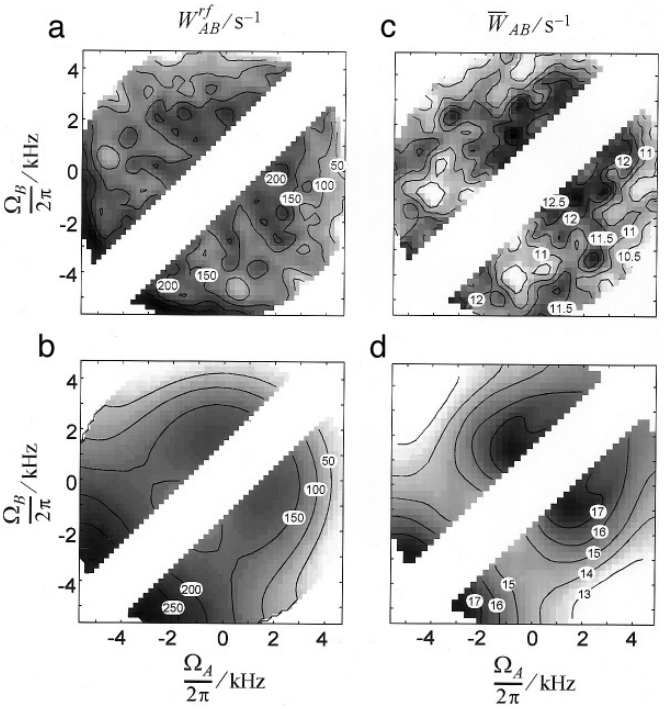

FIG. 4. Rate constants of RF-driven and S-MAS polarization transfer between the two carboxylic carbons in phthalic acid as a function of the resonance frequencies Ω_A and Ω_B. (a) Experimental rate constants obtained from RF-driven polarization-transfer experiments using the WALTZ17 sequence. The rate constants were measured from a fit to a straight line of the time dependence of the off-diagonal intensities in the initial rate regime scaled by the respective intensities of the quasi-equilibrium spectrum. Six experiments were used with mixing times increasing from 0 to 2.5 ms in 0.5-ms steps. For each pair of resonance frequencies, only cross-peak intensities below half of the respective quasi-equilibrium value were considered. The decay of the spin-locked magnetization during the mixing time was negligible. (b) Best fit of the distribution of the rate constants shown in (a). The angle Ψ of the rotation of the principal axis system of the carboxylic ^{13}C CSA tensor about the twofold symmetry axis (see Fig. 3) and the intensity of the ZQ spectrum at frequency zero $F^{RF}(0)$ were optimized. The results are $\Psi = 4.9° \pm 7.0°$ and $F^{RF}(0) = (1.98 \pm 0.01) \times 10^{-4}$ s. (c) Experimental rate constants obtained from S-MAS polarization-transfer experiments. The rate constants were measured from four experiments with mixing times 0, 10, 20, and 30 ms as mentioned in (a). Longitudinal relaxation during the mixing time was negligible. (d) Rate constants of polarization transfer under S-MAS calculated from the crystal structure and the intensities of the ZQ spectrum. The ZQ intensities were obtained from cross-products of two proton-coupled one-quantum spectra.

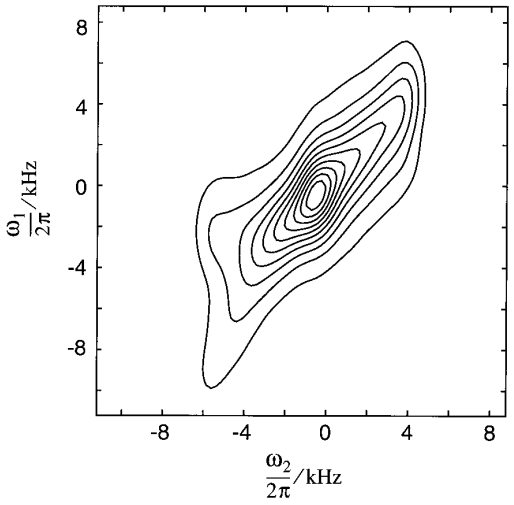

FIG. 5. Experimental 2D separated-local-field spectrum of the carboxylic carbons in phthalic acid. The one-quantum spectra, resolved according to the chemical shifts, can be obtained from sections along ω_1.

sured by X-ray (*28*). The regions of low and high rate constants in the two data sets coincide well, but the relative deviations from the respective mean value are larger for the calculated rate constants. The smaller experimental mean value and the smaller experimental variations compared to those calculated are, at least partially, due to deviations from the initial rate regime, where the off-diagonal intensities are assumed to increase linearly with the mixing time.

If the rate constants are calculated by averaging the geometrical part and the spectral part separately in Eq. [6], $\langle\overline{(3\cos^2(\theta_{ij})-1)^2}\rangle_{AB}\langle\overline{F_{ij}^H(0)}\rangle_{AB}$, the resulting values differ from those in Fig. 4d by less than 2%. Furthermore, the variations of $\langle\overline{F_{ij}^H(0)}\rangle_{AB}$ as a function of the resonance frequencies Ω_A and Ω_B are below 4%. Therefore, most of the variations of the rate constants in Fig. 4d are due to an incomplete averaging under S-MAS of the dependence of the rate constants on the angular part of the dipolar coupling.

To obtain a more general understanding of the averaging of polarization transfer under S-MAS, rate constants were calculated for different relative orientations of the CSA tensors and different orientations of the internuclear vector. These calculations show that the variations of the rate constant $\bar{W}_{AB}$ depends on the relative orientations of the internuclear vector and the CSA tensors. However, over the whole frequency range, the maximal deviation from the mean value remains almost constant, slightly below $\pm 20\%$. For the typical situation where the width of the ZQ line is on the same order as the range covered by the resonance frequencies, this is a good estimation of the maximal error made when using Eq. [7] to establish a relationship between the structure and the rate constants of polarization transfer. Even when the width of the ZQ line is more than one order of magnitude narrower than the resonance-frequency range, the variations of the rate constants increased only up to $\pm 25\%$. It is important to note that if different orientations of the internuclear vector exist for the same relative orientation of the two CSA tensors, the error will be substantially lower than that given above. Such geometries are expected in amorphous systems.

The two polarization-transfer techniques can be compared on the basis of the differences between the rate constants in Figs. 4a and 4c. On average, the RF-driven technique can transfer spin order faster. However, the duration of the transfer is limited by the decay of the spin-locked polarization, while under S-MAS the longest transfer time is set by the longitudinal relaxation of the magnetization.

Both techniques can be used to study local order in polycrystalline or amorphous solids. The RF-driven technique preserves the sensitivity of the rate constants to the orientation of the vector between the correlated nuclei in the molecular frame. In contrast, the S-MAS technique offers the possibility to study orientational correlation as a function of the distance only. This can be especially useful for studying local order in amorphous solids. If $P(\alpha, \beta, \gamma, r)$ defines the probability of finding two groups whose distance is r and whose relative orientation is given by the Euler angles (α, β, γ), the weighted probability integrated over the whole distance range, $\bar{P}(\alpha, \beta, \gamma) = \int P(\alpha, \beta, \gamma, r) r^{-6} dr$, might be reconstructed from the rate constants. Such probability distribution would provides direct information about local order even if a detailed molecular model is not available.

If the explicit dependence of the rate constants on the orientation of the vector between the spins is not desired, three aspects speak in favor of the S-MAS technique. First, the broadening of the energy levels of the S spins by the nearby protons is usually much larger than the dipolar interactions among the S spins, so that perturbation theory, leading to Eq. [1] (*23, 24*), can be safely applied. Second, polarization transfer under S-MAS is hardly sensitive to the ZQ linewidth (*18*). Therefore, errors made by approximating the ZQ spectrum by the cross-product of two 1Q spectra have little effect on distances obtained from rate constants of polarization transfer under S-MAS. Third, the S-MAS technique can easily be used to study systems with a resonance-frequency spread of many tens of kilohertz on standard commercial spectrometers, while the investigation of such systems with the RF-driven technique would require RF fields much stronger than 100 kHz.

CONCLUSION

The comparison of rate constants in a model system has demonstrated a major difference between RF-driven and S-MAS polarization transfer. While both techniques can render the transfer of polarization independent of resonance frequency, they lead to different dependences of the rate constants on the orientation of the internuclear vector with re-

spect to the static magnetic field. On the one hand, the RF-driven technique preserves the dependence as it obtains in static samples. For simple systems, this dependence can provide information about the orientation of the CSA tensors with respect to a molecule fixed frame. On the other hand, the S-MAS technique strongly attenuates this dependence and yields averaged rate constants which depend almost exclusively on the distance between the spins. This simplification can be useful in the study of complex systems like amorphous polymers.

ACKNOWLEDGMENTS

We thank Professor R. R. Ernst for valuable comments on the manuscript. This work was supported by the Swiss National Science Foundation.

REFERENCES

1. R. A. Assink, *Macromolecules* **11,** 1233 (1978).
2. J. Virlet and D. Ghesquires, *Chem. Phys. Lett.* **73,** 323 (1980).
3. P. Caravatti, J. A. Deli, G. Bodenhausen, and R. R. Ernst, *J. Am. Chem. Soc.* **104,** 5506 (1982).
4. R. Tycko and G. Dabbagh, *J. Am. Chem. Soc.* **113,** 3592 (1991).
5. R. Tycko and G. Dabbagh, *Mater. Res. Soc. Symp. Proc.* **215,** 125 (1991). R. Tycko and G. Dabbagh, *Isr. J. Chem.* **32,** 179 (1992).
6. G. Dabbagh, D. P. Weliky, and R. Tycko, *Macromolecules* **27,** 6183 (1994).
7. R. Tycko, D. P. Weliky, and A. E. Berger, *J. Chem. Phys.* **105,** 7915 (1996).
8. P. Robyr, B. H. Meier, and R. R. Ernst, *Chem. Phys. Lett.* **187,** 471 (1991).
9. P. Robyr, B. H. Meier, P. Fischer, and R. R. Ernst, *J. Am. Chem. Soc.* **116,** 5315 (1994).
10. P. Robyr, M. Tomaselli, J. Straka, C. Grob-Pisano, U. W. Suter, B. H. Meier, and R. R. Ernst, *Mol. Phys.* **84,** 995 (1995).
11. P. Robyr, M. Tomaselli, C. Grob-Pisano, B. H. Meier, R. R. Ernst, and U. W. Suter, *Macromolecules* **28,** 5320 (1995).
12. B. H. Meier, *Adv. Magn. Opt. Reson.* **18,** 1 (1994).
13. A. E. Bennet, R. G. Griffin, and S. Vega, *NMR Basic Principles Prog.* **33,** 1 (1994).
14. H. T. Edzes and J. P. C. Bernards, *J. Am. Chem. Soc.* **106,** 1515 (1984).
15. P. M. Henrichs and M. Linder, *J. Magn. Reson.* **58,** 458 (1984).
16. R. R. Ernst, G. Bodenhausen, and A. Wokaun, ''Principles of Nuclear Magnetic Resonance in One and Two Dimensions,'' Clarendon, Oxford (1987).
17. P. Robyr, B. H. Meier, and R. R. Ernst, *Chem. Phys. Lett.* **162,** 417 (1989).
18. Z. Gan and R. R. Ernst, *Chem. Phys. Lett.* **253,** 13 (1996).
19. A. J. Shaka, J. Keeler, and R. Freeman, *J. Magn. Reson.* **53,** 313 (1983).
20. D. P. Burum, M. Linder, and R. R. Ernst, *J. Magn. Reson.* **53,** 394 (1983).
21. K. Tagegoshi, I. Mitsuru, and T. Terao, *Chem. Phys. Lett.* **260,** 159 (1996).
22. Z. Gan, P. Robyr, and R. R. Ernst, *Chem. Phys. Lett.* **283,** 262 (1998).
23. A. Abragam, ''Principles of Nuclear Magnetism,'' Clarendon, Oxford (1961).
24. D. Suter and R. R. Ernst, *Phys. Rev. B* **32,** 608 (1985).
25. A. Kubo and C. A. McDowell, *J. Chem. Phys.* **89,** 63 (1988).
26. R. K. Hester, J. L. Ackerman, B. L. Neff, and J. S. Waugh, *Phys. Rev. Lett.* **36,** 1081 (1976); E. F. Rybaczewski, B. L. Neff, J. S. Waugh, and J. S. Sherfinski, *J. Chem. Phys.* **67,** 1231 (1977).
27. W. Nowacki and H. Jaggi, *Z. Kristallogr.* **109,** 272 (1957).
28. O. Ermer, *Helv. Chim. Acta* **64,** 1902 (1981).
29. M. Mehring, ''High Resolution NMR in Solids,'' Springer-Verlag, Heidelberg (1983).
30. W. S. Veeman, *Prog. NMR. Spectrosc.* **16,** 193 (1984).
31. C. E. Bronniman, N. M. Szeverenyi, and G. E. Maciel, *J. Chem. Phys.* **79,** 3694 (1983).
32. D. L. VanderHart, *J. Magn. Reson.* **72,** 13 (1987).